Two Regimes of the Kitaev Materials: Li_2RhO_3 and $Ag_3LiRh_2O_6$

Xiaodong Hu*
Department of Physics, Boston College
(Dated: June 5, 2021)

In this note, with the help of density-functional calculation and Hartree-Fock mean-field data, we build the low-energy effective Hamiltonians for two generation of Kitaev materials Li_2RhO_3 (LRO) and $Ag_3LiRh_2O_6$ (ALRO). We show that LRO is controlled by the physics of strong spin-orbital coupling while ALRO is dominant by a trigonal distortion. Particularly, taking SOC as perturbation, we argue that the low-energy manifold of ALRO is Kramers doublet, and the low-energy Hamiltonian will contain exchanges of Ising-anisotropy. Furthermore, except for the common effects originating from spin-orbital coupling (SOC) and trigonal distortion, we notice that there is another geometric distortion that breaks the RhO_4 coplane condition. Such distortion is neglegible for ALRO but commensurable in LRO, leading the low-energy exchange of LRO deviating from the Kitaev Hamiltonian.

尽挹西江，细斟北斗，万象为宾客。扣舷独啸，不知今夕何夕。

—— 张孝祥「水调歌头」

Contents

I. LOW-ENERGY EFFECTIVE HAMILTONIAN

A general strongly-interacting Hubbard-like Hamiltonian with rotational-invariant spin-spin interaction and arbitrary orbital degrees of freedom can be written as

$$H = J_1 \sum_{\langle ij \rangle} \boldsymbol{S}_i \cdot \boldsymbol{S}_j + \sum_{\langle ij \rangle} J^{\alpha\beta}_{2,ij} \tau^\alpha_i \tau^\beta_j + \sum_{\langle ij \rangle} J^{\alpha\beta}_{3,ij} (\boldsymbol{S}_j \cdot \boldsymbol{S}_j)(\tau^\alpha_i \tau^\beta_j) + \cdots . \tag{1}$$

Since there may be anisotropic terms for the orbital part of exchange like $\tau^z_i \tau^z_j, \tau^x_i \tau^x_j, \tau^x_i \tau^y_i$, etc., the general Hamiltonian (1) is really intractable for theoretical analysis. However, with the help of crystalline symmetry, in real materials many terms turn out to be vanishing. Particularly, we will show at the end of this section that, for ALRO, the allowed low-energy Hamiltonian can only be composed of Ising-like exchanges.

*Electronic address: xiaodong.hu@bc.edu

A. Octahedral Crystal Field

It is well-known in crystal field theory [1] that the spherical symmetric $3d$-orbitals will split into two-fold e_g orbitals (omitting the irrelevant radial part)

$$|d_{x^2-y^2}\rangle = \frac{1}{\sqrt{2}}(Y_2^{-2} + Y_2^2), \quad |d_{3z^2-r^2}\rangle = Y_2^0,$$

and three-fold t_{2g} orbitals

$$|d_{zx}\rangle = \frac{1}{\sqrt{2}}(Y_2^{-1} - Y_2^1), \quad |d_{yz}\rangle = \frac{i}{\sqrt{2}}(Y_2^{-1} + Y_2^1), \quad |d_{xy}\rangle = \frac{i}{\sqrt{2}}(Y_2^{-2} - Y_2^2),$$

in the octahedral oxygen environment, with $Y_\ell^m(\theta, \phi)$ the familiar spherical harmonics, as is shown in FIG. 1.

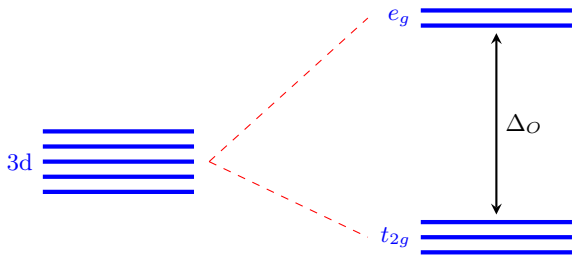

FIG. 1: **Octahedral Crystal Field Splitting.**

Depending on the energy scale between such e_g-t_{2g} splitting Δ_O and Hubbard U and Hund's coupling J_H (with a realistic relation $U > J_H$), we will fall into either high-spin or low-spin states with the electron configuration $3d^5$ of Rh^{3+}. When $U > J_H \gg \Delta_O$, the interplay of onsite electron-electron repulsion and Hund's rule will lead to a configuration of half-filling of *both* t_{2g} and e_g orbitals at the first place. And the last one electron will be placed on the four-fold degenerate t_{2g} orbitals, leaving us in the high-spin state. In contrast, if the energy scale of e_g-t_{2g} splitting is prominent (or at least comparable with Hubbard U and Hund's J_H) $\Delta_O \gtrsim U > J_H$, then these five electrons will try to occupy the six-fold degenerate (including spin degeneracy) t_{2g} orbitals first, leaving only one empty hole. So we are in the low-spin state.

To determine which one is the case, we can simply take a look at the numerical energy spectrum of relevant ten orbitals. Based on the DFT calculation of LRO and ALRO, we extract a wannierized tight-binding model with the input (by-hand) interactions (containing Hubbard U and Hund's J) and SOC. Although there is no pre-knowledge on these parameters, as an energy scale estimation it is enough to take their values from Rh's atomic properties of $3d$-orbitals. For example, we can simply use the experimental results [2] to add SOC with the coupling constant $\lambda_d = 0.114$. And Hund's J_H can be determined with the Rh's atomic slater-condon interaction parameters (I have no idea about this) [3]

$$J_H \equiv \frac{S}{14}(F^2(3d;3d) + F^4(3d;3d)), \quad F^2(3d;3d) = 0.282 \times 27.2, \quad F^4(3d;3d) = 0.182 \times 27.2,$$

with some material screening factor $S \sim 0.8$. For Hubbard U representing the e-e Coulomb interaction, however, we cannot ignore the many-body effect anymore, but can only determine it with the comparison of the optical gap observed in experiments. Given a Hubbard U, the numerical optical gap can be obtained by self-consistent running of Hartree-Fork approximation. After a serials of trials, we will take the $U \sim 3.0$ for both LRO and ALRO, matching the optical gap to be around 650mV.

With all parameters set, now the energy spectrum can be obtained by diagonalization of the quadratic tight-binding Hamiltonian (obtained with Hartree-Fork mean-field method). The relevant results (with SOC on and off) are listed in TABLE. I.

Although the existence of SOC slightly shift both ten energy levels, the e_g-t_{2g} splitting gap $\Delta_O^{\text{LRO}} \simeq 2.94756$eV and $\Delta_O^{\text{ALRO}} \simeq 3.0345$eV are in commensurate with Hubbard $U \sim 3.0$. So we can safely conclude that the discussion of low-energy physics can be confined in the subspace of t_{2g} orbitals only.

There is a well-known phenomena called t_{2g}-p *equivalence* [4] stating that the *effective* angular momentum within t_{2g} subspace quenches to have a similar form of that on p-orbitals

$$\mathbf{L}|_{t_{2g}} = -\mathbf{L}|_p. \tag{2}$$

	LRO without SOC	LRO with SOC
t_{2g}	8.72285690310658	8.67598932812092
	8.72285690310658	8.675989328120933
	8.752896854397369	8.730099641245802
	8.752896854397376	8.730099641245813
	8.819499295755385	8.884903534921547
	8.819499295755387	8.88490353492155
e_g	11.635763926129755	11.642613587390171
	11.635763926129762	11.642613587390173
	11.789525861249246	11.79621047265392
	11.789525861249246	11.796210472653923

	ALRO without SOC	ALRO with SOC
t_{2g}	9.166541771379567	9.142025045656869
	9.166541771379569	9.142025045656881
	9.42234146297424	9.371810987827514
	9.422341462974245	9.371810987827523
	9.436907961253517	9.50713680312438
	9.436907961253526	9.507136803124386
e_g	12.329049772638278	12.336116219990881
	12.329049772638282	12.336116219990888
	12.406462151678134	12.413564910334824
	12.406462151678145	12.41356491033483

TABLE I: Energy Spectrum of $3d$ Orbitals for both LRO and ALRO with/without SOC.

This can be seen more clearly by rotating the aforementioned basis of t_{2g}-subspace to

$$|+1\rangle \equiv \frac{1}{\sqrt{2}}(|d_{zx}\rangle - i|d_{yz}\rangle) = Y_2^{-1}, \quad |0\rangle \equiv i|d_{xy}\rangle = \frac{1}{\sqrt{2}}(Y_2^2 - Y_2^{-2}), \quad |-1\rangle \equiv \frac{1}{\sqrt{2}}(|d_{zx}\rangle + i|d_{yz}\rangle) = -Y_2^1.$$

and express the 5×5 matrix of angular-momentum operator in the basis of $\{|+1\rangle, |0\rangle, |-1\rangle, |d_{3z^2-y^2}\rangle, |d_{x^2-y^2}\rangle\}$

$$L_x = -\frac{1}{\sqrt{2}}\left(\begin{array}{ccc|cc} 0 & 1 & 0 & -\sqrt{3} & -1 \\ 1 & 0 & 1 & 0 & 0 \\ 0 & 1 & 0 & \sqrt{3} & 1 \\ \hline -\sqrt{3} & 0 & \sqrt{3} & 0 & 0 \\ -1 & 0 & 1 & 0 & 0 \end{array}\right),$$

$$L_y = -\frac{i}{\sqrt{2}}\left(\begin{array}{ccc|cc} 0 & 1 & 0 & \sqrt{3} & 1 \\ -1 & 0 & 1 & 0 & 0 \\ 0 & -1 & 0 & \sqrt{3} & -1 \\ \hline -\sqrt{3} & 0 & -\sqrt{3} & 0 & 0 \\ 1 & 0 & 1 & 0 & 0 \end{array}\right),$$

$$L_z = -\left(\begin{array}{ccc|cc} 1 & 0 & 0 & 0 & 0 \\ 0 & 0 & 0 & 0 & -2 \\ 0 & 0 & -1 & 0 & 0 \\ \hline 0 & 0 & 0 & 0 & 0 \\ 0 & -2 & 0 & 0 & 0 \end{array}\right).$$

Clearly within the subspace of t_{2g} (3×3 block), the angular mometum operator takes exactly the form of that on the $\ell = 1$ p-orbitals (off-diagonal components can be ignored due to the large gap Δ_O). While within the subspace of e_g (2×2 block), $\mathbf{L}|_{e_g} \equiv 0$ and the further SOC are *quenched*.

But this is not the end of the story. Due to the competition between SOC and geometric distortion (here is trigonal distortion), we will end up with more fine structure of energy splitting within t_{2g} orbitals, as may be already noticed in TABLE I. In fact, we will see below that **LRO and ALRO fall exactly into the two regimes of such competition: for LRO the SOC is dominant (with trigonal distortion negligible), while for ALRO the trigonal distortion is dominant (with SOC taken as perturbations).** We will see that extra quenching of the effective angular momentum operator with t_{2g} subspace (as well as extra splitting) occurs if we further take into account the SOC (as perturbation) in ALRO.

B. Strong Spin-Orbital Coupling

When spin-orbital coupling (we denote $\boldsymbol{L}|_{t_{2g}} \equiv \boldsymbol{l}_{\text{eff}}$)

$$H_{\text{SOC}} = \lambda \sum_{\langle i,j\rangle} \boldsymbol{l}_{\text{eff},i} \cdot \boldsymbol{S}_j \tag{3}$$

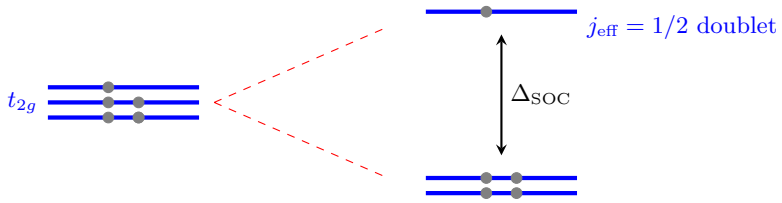

FIG. 2: **Splitting from SOC.**

is dominant, which is the case for LRO, clearly the t_{2g} triplet $l_{\text{eff}} = 1$ and $S = 1/2$ gives the $j = 1/2$ doublet as the ground state, as is shown in FIG. 2. The small splitting energy $\Delta_{\text{SOC}} \simeq 0.0816\text{eV}$ can be read from TABLE I.

The superexchange can then be projected to such subspace through a $\tau = 1/2$ pseudospin operator. The effective Hamiltonian for strongly localized electrons ($U > J_H \gg t$) has already been well-studied for perovskites with 180° exchange, e.g., Sr_2IrO_4, and 90° exchange, i.e., Na_2IrO_3, in [5]. Since in LRO the RhO_6 octahedra is edge-sharing, Jackeli and Khaliullin's result shows that the effective Hamiltonian is Kitaev-like [6]

$$H = -J \sum_{\langle ij \rangle} \mathcal{H}_{ij}^{(\gamma)} = -J \sum_{\langle ij \rangle} S_i^{\gamma} S_j^{\gamma}, \tag{4}$$

where $\gamma = \{x, y, z\}$ labeling the types of ij-bonds.

C. Strong Trigonal Distortion with SOC as Perturbation

In reality, chances are the RhO_6 octahedra to be compressed or stretched along $\hat{z}$ axis. Such trigonal crystal field breaks the t_{2g} triplet into an a_{1g} singlet [7]

$$|a_{1g}\rangle \equiv |d_{3z^2-r^2}\rangle,$$

and e_g' doublet

$$|e'_{g1}\rangle \equiv \frac{2}{\sqrt{6}}|d_{xy}\rangle - \frac{1}{\sqrt{3}}|d_{zx}\rangle, \quad |e'_{g2}\rangle \equiv \frac{2}{\sqrt{6}}|d_{x^2-y^2}\rangle - \frac{1}{\sqrt{3}}|d_{yz}\rangle,$$

which is the case for our ALRO, as is show in FIG. 3. This time the energy splitting is a little bit larger $\Delta_T = 0.2630\text{eV}$.

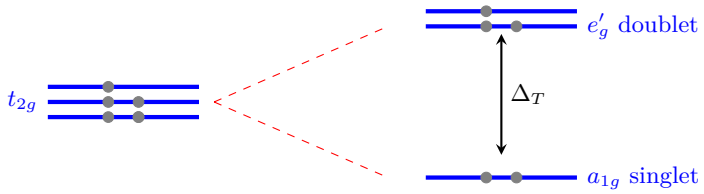

FIG. 3: **Splitting from Trigonal Distortion.**

Although it is tempting to pop up the idea that the effective orbital momentum is $l_{\text{eff}}|_{e_g'} = 3/2$ at a first glance of the four-fold degenerate e_g' orbitals in FIG. 3, a careful representation of $\boldsymbol{l}_{\text{eff}}$ in the new basis of $\{|a_{1g}\rangle, |e'_{g1}\rangle, |e'_{g2}\rangle\}$ tells you NOT. In fact, the t_{2g} effective orbital momentum operator now takes a strange form of

$$l_{\text{eff},x} = \left(\begin{array}{c|cc} 0 & \cdots & \\ \hline \vdots & 0 & 0 \\ & 0 & 0 \end{array}\right), \quad l_{\text{eff},y} = \left(\begin{array}{c|cc} 0 & \cdots & \\ \hline \vdots & 0 & 0 \\ & 0 & 0 \end{array}\right), \quad l_{\text{eff},z} = \frac{1}{3}\left(\begin{array}{c|cc} 0 & \cdots & \\ \hline \vdots & 0 & -i \\ & i & 0 \end{array}\right). \tag{5}$$

Again due to the comparable large gap Δ_T, we can safely narrow our discussion in the subspace of e_g' orbitals, giving the only non-vanishing component of angular momentum matrix

$$l_{\text{eff},z}|_{e_g'} \propto \begin{pmatrix} 0 & -i \\ i & 0 \end{pmatrix} \equiv \tau^y, \tag{6}$$

which is *odd* under time-reversal (TR) symmetry (while τ^x and τ^z are TR *even*).

Now since orbital degree of freedom are described by the set of 2×2 matrices $\{\tau^x, \tau^y, \tau^z\}$, the requirement of on-site TR symmetry drastically reduces the most general form of the effective Hamiltonian (1) into

$$H_{\text{eff}} = J_1 \sum_{\langle ij\rangle} \boldsymbol{S}_i \cdot \boldsymbol{S}_j + \sum_{\langle ij\rangle} \sum_{(\alpha,\beta)\in\mathcal{I}} J_{2,ij} \tau_i^\alpha \tau_i^\beta + \sum_{\langle ij\rangle} \sum_{(\alpha,\beta)\in\mathcal{I}} J_{3,ij} (\boldsymbol{S}_i \cdot \boldsymbol{S}_j)(\tau_i^\alpha \tau_j^\beta), \tag{7}$$

with the allowed index set of orbital exchanges ($\tau^0 \equiv \mathbb{1}$)

$$\mathcal{I} = \{(x,x),(y,y),(z,z),(x,0),(z,0),(x,z)\}.$$

Here exchanges like $\tau_i^x \tau_j^y$ and $\tau_i^y \tau_j^z$ are excluded since they are all time-reversal *odd*.

The above discussion only include the effects from trigonal distortion. Now if we take the SOC as a perturbation, which is the case for ALRO, by adding (7) with (all other components like $\lambda \tau^x S^x$ are TR odd so suppressed in projection into the e_g' subspace)

$$H_{\text{SOC}} = \lambda \sum_{\langle ij\rangle} \tau_i^y S_j^y, \tag{8}$$

then clearly the low-energy state is of *two-fold* degenerate

$$|\mu_z = 1\rangle \equiv |\tau_y = 1, S_z = 1/2\rangle, \quad |\mu_z = -1\rangle \equiv |\tau_y = -1, S_z = -1/2\rangle, \tag{9}$$

forming a Kramers doublet.

Since such energy choice of Kramers doublet (9) is fixed, there would be NO rotation symmetry for the effective Hamiltonian within the final low-energy subspace $\{|\mu_z = \pm 1\rangle\}$. The allowed two-body exchange we can write down will manifestly exhibit an *Ising-anisotropy*,

$$H_{\text{eff}} = \sum_{\langle ij\rangle} \sum_{\alpha\neq\beta} \mu_i^\alpha \mu_j^\beta + A \sum_{\langle ij\rangle} \mu_i^x \mu_j^x + B \sum_{\langle ij\rangle} \mu_i^y \mu_j^y + C \sum_{\langle ij\rangle} \mu_i^z \mu_j^z + \cdots. \tag{10}$$

That is why we expect the ground state of ALRO will be in Ising-like phase (at least along one direction), e.g., a zigzag stripe phase. Since the low-energy subspace fixes $S_z = \pm 1/2$, the spin configuration of ALRO will also be easy-axis along $\hat{z}$ direction.

Another measurable effect is that, if we apply an external magnetic field $\boldsymbol{B}$ coupling with both spin and orbital degrees of freedom

$$H_Z = \mu_B(\boldsymbol{\tau} + 2\boldsymbol{S}) \cdot \boldsymbol{B}, \tag{11}$$

the behavior extra energy splitting from SOC will alter with the direction of $\boldsymbol{B}$: for TR *even* external magnetic field $\boldsymbol{B} = B_\perp$ perpendicular to the trigonal axis $\hat{z}$, the orbital contribution of Zeeman coupling can only takes the form of $H_Z^{\text{orbital}} \sim B_\perp \tau^{x,z}$, while the spin-orbital coupling (8) possesses only y-component. So there would be no interplay of H_{SOC} and H_Z and no extra splitting occurs when $B_\perp$ is applied. However, for the TR *odd* external magnetic field along the trigonal axis $\boldsymbol{B} = B_\parallel$, the only possible combination of the orbital-part of the Zeeman couling takes the form of $H_Z^{\text{orbital}} \sim B_\parallel \tau^y$, which does interplay with SOC so further splitting of the energy levels within the $\{|\mu_z = \pm 1\rangle\}$ subspace occurs. Similar discussion is applied with $M\text{PS}_3$ ($M = \text{Mn, Fe and Ni}$) in [8].

D. Extra Distortion

As is shown in the numerical TABLE I, except for the above discussions of SOC and trigonal distortions, the fully-filled $j = 3/2$ quadruplet of t_{2g} orbitals are actually not perfectly degenerate. There exists an extra mechanism splitting them, with a tiny gap about $\Delta_E^{\text{LRO}} \simeq 0.03$eV, which is quite comparable with Δ_{SOC} (about 36.7%). A similar splitting occurs in ALRO, but the energy scale $\Delta_E^{\text{ALRO}} \simeq 0.0146$eV is much smaller in comparison with Δ_T (about merely 5.56%).

This can be ascribed to the extra distortion we find on the wannier centers of RhO_6 octahedron: For the octahedron with merely trigonal distortion, the RhO_4 plane should keep coplane. But a visualization of wannier centers evidently exhibit a violation of such coplane condition, as shown in FIG. 4.

In light of this extra distortion, the Khaliullin's requirement of a *strong* SOC may not be satisfied in LRO, and their effective Kitaev Hamiltonian may also not be accurate. While for ALRO we believe that the above low-energy analysis won't be altered.

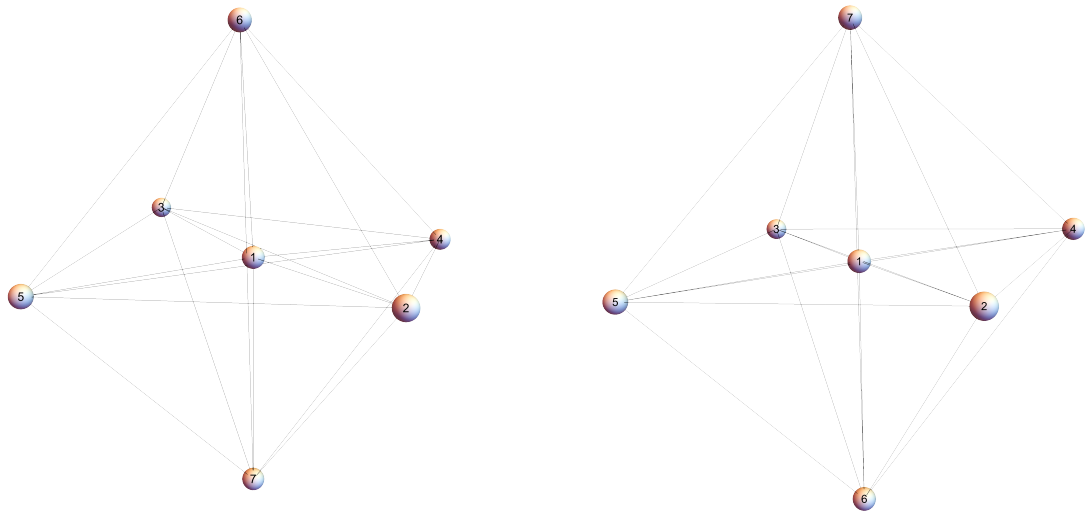

FIG. 4: **Wannier Centers of LRO and ALRO**: The left graphics is for LRO, while the right one is for ALRO. We draw the diagonal line to compare with the O-Rh-O plane. The discrepancy is in accordance with the strength of extra energy splitting we found in numerical results. Thus the extra distortion is much stronger in LRO than that for ALRO.

II. LONG-RANGE ORDER

A. LRO

B. ALRO

[1] P. Fazekas, *Lecture notes on electron correlation and magnetism*, vol. 5 (World scientific, 1999).
[2] M. Blume and R. Watson, Proceedings of the Royal Society of London. Series A. Mathematical and Physical Sciences **271**, 565 (1963).
[3] J. C. Slater, Physical Review **34**, 1293 (1929).
[4] S. Sugano, *Multiplets of transition-metal ions in crystals* (Elsevier, 2012).
[5] G. Jackeli and G. Khaliullin, Physical review letters **102**, 017205 (2009).
[6] A. Kitaev, Annals of Physics **321**, 2 (2006).
[7] S. Landron and M.-B. Lepetit, Physical Review B **77**, 125106 (2008).
[8] P. Joy and S. Vasudevan, Physical Review B **46**, 5425 (1992).